Magnetic state effect upon the order-disorder phase transition in Fe-Co alloys: A first-principles study

Moshiour Rahaman,[1,2] A. V. Ruban,[1] Abhijit Mookerjee,[3] and B. Johansson[1]

[1]*Applied Material Physics, Department of Materials Science and Engineering, Royal Institute of Technology, SE-100 44 Stockholm, Sweden*
[2]*Department of Materials Science, S.N. Bose National Centre for Basic Sciences, JD Block, Sector III, Salt Lake City, Kolkata 700098, India*
[3]*Advanced Materials Research Unit, S.N. Bose National Centre for Basic Sciences, JD Block, Sector III, Salt Lake City, Kolkata 700098, India*

(Received 8 November 2010; published 7 February 2011)

We investigate the effect of global magnetization on the effective cluster interactions and order-disorder phase transition in Fe_xCo_{1-x} alloys. The effective cluster interactions are obtained by the screened generalized perturbation method as it is implemented in the exact muffin-tin orbitals formalism within the coherent potential approximation. The ordering transition from the high-temperature disordered body-centered cubic alloy to the ordered $B2$ phase is determined by Monte Carlo simulations. The calculated transition temperatures are in good agreement with the available experimental data for the effective interactions, which correspond to the experimentally observed magnetization at the order-disorder phase transition.

DOI: 10.1103/PhysRevB.83.054202 PACS number(s): 75.50.Bb, 64.90.+b, 71.20.Be, 71.55.Ak

I. INTRODUCTION

Fe-Co alloys possess a unique combination of magnetic and mechanical properties, which make them indispensable as materials for advanced motors and electrical generators in aviation and special power applications.[1] In particular, they are characterized by exceptionally high saturation magnetization, low coercivity, and high Curie temperature (>1093 K). The elevated Curie temperatures of the alloys make them especially attractive for various high-temperature applications. However, at around 1003 K, the disordered body-centered cubic (bcc) Fe_xCo_{1-x} alloys undergo an ordering phase transition into the $B2$ structure (space group Pm3m) in the composition range $\sim 0.3 \leqslant x \leqslant 0.7$,[2–5] which significantly affects their magnetic and mechanical properties.

There exist numerous investigations of phase equilibria in the Fe-Co system; in particular, the order-disorder phase transition.[3] This has been observed by Seehra and Silinsky,[2] who measured the electrical resistivity in Fe-Co alloys and found, near $T_c = 1006$ K, a change in the slope of the temperature-dependent resistivity curve indicating an order-disorder phase transition. Oyedele and Collins[3] investigated the order-disorder phase transition in Fe-Co alloys by the neutron powder diffraction techniques for the concentration range of 0.3 to 0.7 of Co. Montano and Seehra[4] used Mössbauer spectroscopy to identify the order-disorder phase transition. They found the transition temperature at about $T_c = 1006$ K for the equiatomic composition. Ohnuma *et al.*[6] investigated the phase equilibria in the Fe-Co system both experimentally, using transmission electron microscopy for thin-film samples and x-ray and electron diffractometer for the bulk system, and theoretically by the CALPHAD method, which was modified by considering chemical interactions dependent on the magnetic state.

The coupling of magnetism and atomic short-range order (SRO) in Fe-Co, up to a concentration 0.25 of Co, has been investigated experimentally by Pierron-Bohnes *et al.*[7–9] using neutron diffuse scattering and nuclear magnetic resonance techniques. The influence of the magnetism on the atomic SRO was clearly evident from an abrupt change in the temperature dependence of the local order at the Curie temperature. The theoretical analysis of the coupling between the magnetic and chemical degrees of freedom based on the mean-field approximation of a combined Ising-Heisenberg Hamiltonian was done by Pierron-Bohnes *et al.*[7] They have shown that the magnetic contribution to the effective interactions should be roughly proportional to the square of the magnetization.

The Fe-Co system has been theoretically studied by using a wide variety of phenomenological methods as well as with first-principles techniques. In an early phenomenological treatment of the $A2$-$B2$ transition, Beinenstock and Lewis[10] employed a low-temperature expansion of the Ising model to calculate a phase diagram with nonmagnetic components. This phenomenological approach resulted in a $B2$ phase field symmetric about the 50-50 composition and somewhat narrower than that found experimentally. A real-space renormalization group was used by Racz and Collins[11] to study the slight asymmetry in the $A2$-$B2$ phase boundary. In the context of a nonmagnetic nearest-neighbor Ising model, they found that a small three-body interaction could account for the experimentally observed asymmetry.

These early phenomenological works did not treat the magnetic transition and effectively hid the effect of magnetism by subsuming it into the effective pair interaction. Other phenomenological works include those by Tahir-Kheli and Kawasaki,[12] Billard *et al.*,[13] Morán-Lopez and Falicov,[14] Mejia-Lira *et al.*,[15] Mizial *et al.*,[16] Sanchez and Lin,[17] and Martinez-Herrera *et al.*[18] They also treated the magnetic transition and demonstrated the interplay between chemical and magnetic interactions in determining the location of chemical phase boundaries. However, in such studies, the chemical interactions for real alloys were obtained from the fitting of simplified models to the experimental properties in the ferromagnetic (FM) state and, thus, could not be applied unambiguously to the nonmagnetic situation. While all of these approaches are able to reproduce various portions of the Fe-Co phase diagram, they are all phenomenological and rely on the thermochemical studies and/or on portions of the experimental phase diagram to obtain the chemical and magnetic interaction parameters.

The method that ideally suits the investigation of the coupling between the chemical and magnetic degrees of freedom at the atomic scale level is the generalized perturbation method (GPM).[19] This method allows for the calculations of both the effective chemical interactions of the Ising Hamiltonian for the atomic configurational degrees of freedom and the magnetic exchange interaction parameters of the Heisenberg Hamiltonian describing magnetic ordering. Bieber and Gautier[20] used this method within an empirical tight-binding approximation to calculate the effect of magnetism on the phase stability in random alloys. Later, Sluiter and Kawazoe[21] used a first-principles-based tight-binding method to calculate effective interactions in binary Fe-Co and ternary Fe-Ni-Al alloys. The calculated order-disorder transition temperature in Fe-Co in the FM state was 600 K, which was way lower than the experimental value of 1006 K. The GPM was also used by Kudrnovský *et al.*[22] in the first-principles calculations of the effective interactions in Fe-Co alloys, both in the bulk and on the surface in the FM state. Their calculated transition temperature in the single-site mean-field approximation was 917 K. Considering the fact that the mean-field approximation actually overestimates the critical temperature, this result can not be considered as satisfactory.

Recently, Diaz-Ortiz *et al.*[23,24] have investigated the possible ground-state structures in Fe-Co alloys using a cluster expansion of the enthalpy of formation determined in first-principles calculations. By also performing nonmagnetic calculations, they have demonstrated that the magnetism has a great impact upon the stability of Fe-Co alloys. As in the previous theoretical considerations, only the fully ferromagnetic state has been considered. However, the point, which still remains missing, is the influence of the finite-temperature magnetic state on the thermodynamics of ordering in this system.

This is the main goal of this investigation. It is based on the partially disordered local moment (PDLM) representation of the finite-temperature magnetic state of Fe-Co alloys. We shall carry out first-principles calculations of the effective cluster interactions and consequently use them in our Monte Carlo simulations. A similar approach has recently been used by Ruban *et al.*[25] and Ekholm *et al.*[26] in the study of Fe-Cr and Fe-Ni alloys, respectively. The main difference, however, is due to a different treatment of the PDLM state, since both alloy components, Fe and Co, exhibit more localized behavior of the magnetic moments.

II. METHODOLOGY

A. Effective cluster interactions for finite magnetization

The PDLM state, which represents the partially ordered magnetic state for a given global magnetization m, can be introduced as a straightforward generalization of the disordered local moment[27,28] (DLM) model. The magnetic binary Fe_xCo_{1-x} alloy is described in terms of a four-component alloy $Fe^{\uparrow}_{ux}Fe^{\downarrow}_{dx}Co^{\uparrow}_{u(1-x)}Co^{\downarrow}_{d(1-x)}$, where $u = (1+m)/2$ and $d = (1-m)/2$, respectively. Fe and Co atoms with up and down spin orientation are distributed randomly relative to one another on the underlying lattice. In the adiabatic approximation adopted in this paper, the dynamics of the spins and its coupling with other types of thermal excitations has been neglected. One can see that this model gives the ferromagnetic state for $m = 1$ and the DLM state for $m = 0$.

Using the fact that thermally induced fluctuations of the local magnetic moment orientations are much faster than the atom-vacancy exchanges associated with equilibrating the atomic short-range order, one can define "spin-averaged" effective pair interactions (EPIs) for a binary Fe_xCo_{1-x} alloy in the PDLM states as[29]

$$\left\langle V_{ij}^{\text{Fe-Co}}\right\rangle = \frac{1}{16}\sum_{\sigma_1,\sigma_2,\sigma_3,\sigma_4} p_{\sigma_1}p_{\sigma_2}p_{\sigma_3}p_{\sigma_4}\bar{V}_{ij}^{\text{Fe}^{\sigma_1},\text{Fe}^{\sigma_2},\text{Co}^{\sigma_3},\text{Co}^{\sigma_4}}, \tag{1}$$

where the summation is over spin orientation index σ for each alloy component. It takes on values $\uparrow$ and $\downarrow$, and the coefficients $p_\sigma = u$ and d for the corresponding spin orientations. $\bar{V}_{ij}^{\text{Fe}^{\sigma_1}\text{Fe}^{\sigma_2}\text{Co}^{\sigma_3}\text{Co}^{\sigma_4}}$ is the generalized EPI for a quaternary alloy for i and j sites, which can be expressed through the ordinary EPIs of binary combinations of the alloy components as[30]

$$\bar{V}_{ij}^{\text{Fe}^{\sigma_1}\text{Fe}^{\sigma_2}\text{Co}^{\sigma_3}\text{Co}^{\sigma_4}} = \tfrac{1}{2}\left(V_{ij}^{\text{Fe}^{\sigma_1}\text{Co}^{\sigma_3}} + V_{ij}^{\text{Fe}^{\sigma_2}\text{Co}^{\sigma_4}} - V_{ij}^{\text{Fe}^{\sigma_1}\text{Fe}^{\sigma_2}} - V_{ij}^{\text{Co}^{\sigma_3}\text{Co}^{\sigma_4}}\right). \tag{2}$$

In the DLM, when $u = d = 0.5$, Eq. (2) takes a simple form

$$V_{ij}^{\text{Fe-Co-DLM}} = \tfrac{1}{4}\left(2V_{ij}^{\text{Fe}^{\uparrow}\text{Co}^{\downarrow}} + 2V_{ij}^{\text{Fe}^{\downarrow}\text{Co}^{\uparrow}} - V_{ij}^{\text{Fe}^{\uparrow}\text{Fe}^{\downarrow}} - V_{ij}^{\text{Co}^{\uparrow}\text{Co}^{\downarrow}}\right), \tag{3}$$

which is rather similar to that of a binary alloy when only one alloy component is magnetic. The last two terms are exchange magnetic interactions of Fe and Co in the DLM state.

The higher-order effective cluster interactions (ECIs) can be determined in a similar way. So, in the end, the configurational Hamiltonian is reduced to the original form for a binary alloy:

$$H_{\text{conf}} = \frac{1}{2}\sum_{i,j} V_{ij}^{(2)}\,\delta c_i\delta c_j + \frac{1}{3}\sum_{i,j,k} V_{ijk}^{(3)}\,\delta c_i\delta c_j\delta c_k + \frac{1}{4}\sum_{i,j,k,\ell} V_{ijk\ell}^{(4)}\,\delta c_i\delta c_j\delta c_k\delta c_\ell. \tag{4}$$

Here, $V_{i_1,\ldots,i_n}^{(n)}$ are the spin average of n-site effective cluster interactions; δc_i are the concentration fluctuations at sites i; and $\delta c_i = c_i - x$, where c_i is the occupation number at site i, taking on values 1 or 0 if the site i is occupied by the Fe or Co atom, respectively. The summation in Eq. (4) is carried out over all sites.

B. Details of the first-principles calculations

We have used three related first-principles techniques for our calculations:

(i) the Korringa-Kohn-Rostoker Green's function method in the atomic sphere approximation (KKR-ASA),[31,32] which was used for the calculation of the densities of states and magnetic moments of the alloys at different compositions;

(ii) the locally self-consistent Green's function (LSGF) method[33,34] based on the KKR-ASA method for the determination of the on-site and intersite screening constants needed for

the electrostatic part of the screened generalized perturbation method (SGPM) effective pair interactions; and

(iii) the exact muffin-tin orbital (EMTO) method within the full charge density formalism[35] for the total energy and cluster interaction calculations.

Randomness has been treated using the coherent potential approximation (CPA)[32,33,36,37]: the KKR-ASA-CPA and the EMTO-CPA. The local density approximation (LDA)[38] has been used for the exchange-correlation potential.

The KKR-ASA Green's function and the LSGF methods have been used to determine the screening constants, which enter the DFT-CPA formalism in the single-site approximation (in the so-called isomorphous CPA model). In this formalism, the on-site screened electrostatic potential $V^i_{\rm scr}$ and energy $E^i_{\rm scr}$ are determined as suggested by Ruban and Skriver[39] and Ruban *et al.*[40]:

$$V^i_{\rm scr} = -e^2\alpha_{\rm scr}\frac{q_i}{S},$$
$$E^i_{\rm scr} = -e^2\frac{1}{2}\alpha_{\rm scr}\beta_{\rm scr}\frac{q_i^2}{S}. \quad (5)$$

Here, q_i is the net charge of the atomic sphere of the ith alloy component, S is the Wigner-Seitz radius, and $\alpha_{\rm scr}$ and $\beta_{\rm scr}$ are the on-site screening constants. Their values, which are $\alpha_{\rm scr} = 0.81, 0.84, 0.88$ and $\beta_{\rm scr} = 1.15, 1.17, 1.18$, have been determined from the corresponding supercell LSGF calculations of random $Fe_{0.3}Co_{0.7}$, $Fe_{0.5}Co_{0.5}$, and $Fe_{0.7}Co_{0.3}$ alloys, respectively.

The screening charge has also been used to determine the intersite screening constants $\alpha_{\rm scr}(R)$ needed in the calculations of the electrostatic part of the SGPM effective pair interactions[39–41] and the intersite screened Coulomb interactions for the i and j sites, which in the case of a binary A-B alloy can be defined as

$$V^{\rm scr}_{ij} = e^2\alpha_{\rm scr}(\mathbf{R}_{ij})\frac{q^2_{\rm eff}}{S}, \quad (6)$$

where $q_{\rm eff} = q_A - q_B$ is the effective charge transfer in the case of a binary alloy and $\mathbf{R}_{ij}$ is the vector connecting sites i and j. The whole SGPM interaction is then

$$V^{(2)}_{ij} = V^{\rm one\text{-}el}_{ij} + V^{\rm scr}_{ij}, \quad (7)$$

where $V^{(2)}_{ij}$ is the SGPM interaction at the ith coordination shell and $V^{\rm one\text{-}el}_{ij}$ is the one-electron contribution to the SGPM interaction.

Experimental lattice parameters[5] have been used in the first-principles calculations of the electronic structure and effective interactions of Fe_xCo_{1-x} alloys. The Monkhorst-Pack grid,[42] with subdivisions along each reciprocal lattice vector $31 \times 31 \times 31$, has been used for integration over the Brillouin zone in the LDA self-consistent and SGPM calculations.

III. RESULTS AND DISCUSSION

A. Electronic structure and magnetic properties of Fe-Co alloy

The electronic structure and magnetic properties of Fe-Co alloys have been calculated previously by MacLaren *et al.*[43] by the KKR-CPA method. In this paper, we use a similar Green's function KKR-ASA-CPA method[31,32] for the calculations of the electron density of states (DOS) and magnetic moments. The experimental[5] lattice spacing varying with composition from $a = 2.835$ to 2.863 Å has been used in our LDA self-consistent calculations.

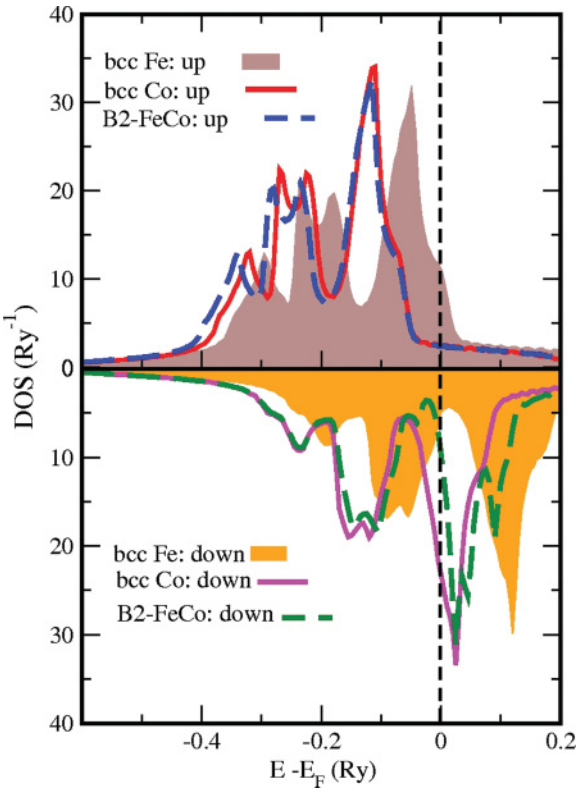

FIG. 1. (Color online) Density of states of bcc Fe, Co, and ordered-$B2$ Fe-Co alloy

In Fig. 1, we show the electronic density of states of pure body-centered-cubic (bcc) Fe and Co as well as the $B2$-ordered Fe-Co alloy calculated for the same lattice parameter $a = 2.86$ Å. The majority bands of pure Fe and Co are shifted relative to each other, which is a consequence of the fact that this band is filled in Co but unoccupied to some degree in Fe. The completely filled majority d band in Co becomes inert or nonbonding and moves down with energy closer to the bottom of the valence band. There is also a substantial difference in the position of the minority band of Co and Fe, which is due to the difference in the number of the occupied states in this band.

What may, however, seem a bit unusual is the fact that the position and the form of the majority and minority bands of the ordered-$B2$ Fe-Co almost coincide with those of bcc Co, almost up to the Fermi energy. Only approximately 3.67 mRy below the Fermi energy, the minority band of Fe-Co becomes different from that of Co by forming an additional valley and redistributing the states above the Fermi energy. To explain the electronic structure of the $B2$ Fe-Co, it is useful to see what happens with electronic states at the local level, inside atomic spheres of Fe and Co.

In Fig. 2(a), we show the local DOS of Co and Fe atoms in the ordered-$B2$ Fe-Co alloy. The local DOS of the majority Fe and Co states are practically the same. The difference in the minority DOS of Fe and Co is more pronounced, although they

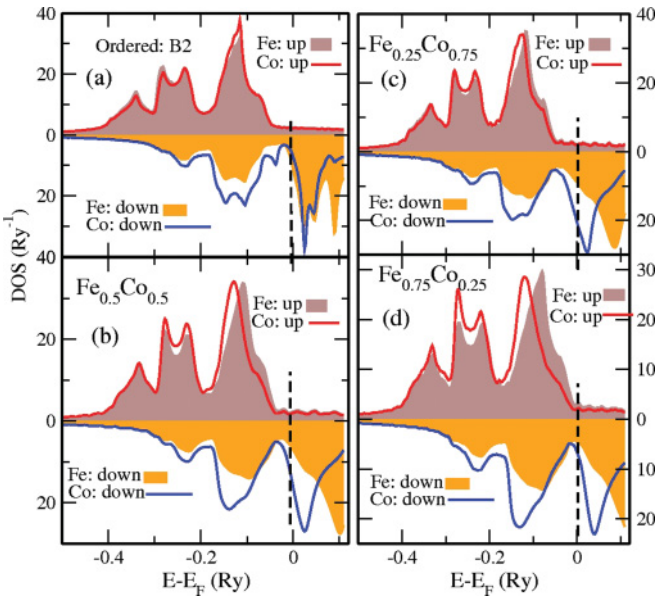

FIG. 2. (Color online) DOS of Fe and Co in ordered-$B2$ and random alloys.

still have a similar form and position up to the Fermi energy. Such a strong similarity of the local Fe and Co bands can be understood, in its turn, in terms of the average bond model, proposed by Ruban *et al.*[44]

Let us note first that the $B2$ structure is quite special in the respect that every Fe atom is completely surrounded by Co atoms at the first coordination shell and vice versa. In this case, the Fe and Co nearest neighbors form a common *bond* between themselves due to the strong hybridization of the d states. Since the d states are quite localized, the influence of more distant coordination shells on the electronic structure is small, and, thus, the DOS of the ordered alloy is very similar to that of pure metals, as has been demonstrated by Ruban *et al.*[44] for the case of nonmagnetic 4d metal alloys. The position of majority and minority states in the $B2$ Fe-Co can be then explained by the shift of the majority d band of Fe-Co due to its complete filling and the consequent hybridization of the minority band with the majority one.

Such a coherent behavior of the local DOS of Fe and Co appears to be disturbed by the randomness in random alloys, which can be clearly seen in Fig. 2(b), where we present the local DOS of a random $Fe_{0.5}Co_{0.5}$ alloy. The positions of the peaks of the local DOS of Fe and Co atoms are shifted relative to each other, which is a manifestation of the fact the they have, on average, an equal number of Fe and Co atoms at the first coordination shell. In particular, the minority DOS of Co strongly increases at the Fermi energy, as it should be when Co atoms have Co nearest neighbors at the first coordination shell (see the DOS of pure Co in the bcc structure in Fig. 1). This makes such an atomic configuration unfavorable compared to the ordered $B2$ structure, and this is the main source origin of the ordering behavior of Fe-Co alloys.

Now, it is easy to understand the reason for the changes of the DOS with variations of the composition of random alloys, which is shown in Figs. 2(c) and 2(d) for $Fe_{0.25}Co_{0.75}$ and $Fe_{0.75}Co_{0.25}$ alloys, respectively. In the case of the $Fe_{0.25}Co_{0.75}$ alloy Fig. 2(c), the average number of Fe atoms surrounding each Fe atom decreases, and the local DOS of Fe mainly follows that of Co, especially in the case of the majority band. At the same time, the average number of Co atoms surrounding each Co atom increases, and this again leads to the increase of the Co minority DOS at the Fermi energy. Conversely, in the case of the $Fe_{0.75}Co_{0.25}$ alloy, the effective number of Fe atoms at the first coordination shell increases, thereby pushing the Fe majority band to the Fermi energy as in pure bcc Fe (see Fig. 1 for Fe). At the same time, Co atoms become surrounded mostly by Fe atoms and this makes it possible to rearrange their minority band in a way to have a valley at the Fermi energy similar to the case of the $B2$ phase.

The concentration dependence of the average magnetic moment of Fe-Co alloys exhibits the Slater-Pauling behavior and it was discussed in detail by MacLaren *et al.*[43] In Fig. 3, we compare our results for the average and local magnetic moments in Fe-Co random alloys with the first-principles calculations by MacLaren *et al.*[43] and experimental data.[45] One can see that our results follow the same trend as MacLaren *et al.*,[43] but closer to the experimental data. The difference arises due to the use of different lattice spacings, since we have used experimental data. Our calculated magnetic moments are a bit lower than the experimental data. The reason for this discrepancy is most probably related to atomic short-range order effects neglected in our single-site CPA calculations, and which may exist and be pronounced in the experimental samples. Let us also note that Co-rich Fe-Co alloys are not good candidates for neutron experiments,[47] first, because of their higher neutron absorption cross section and also because of their high magnetic anisotropy. Fe-Co

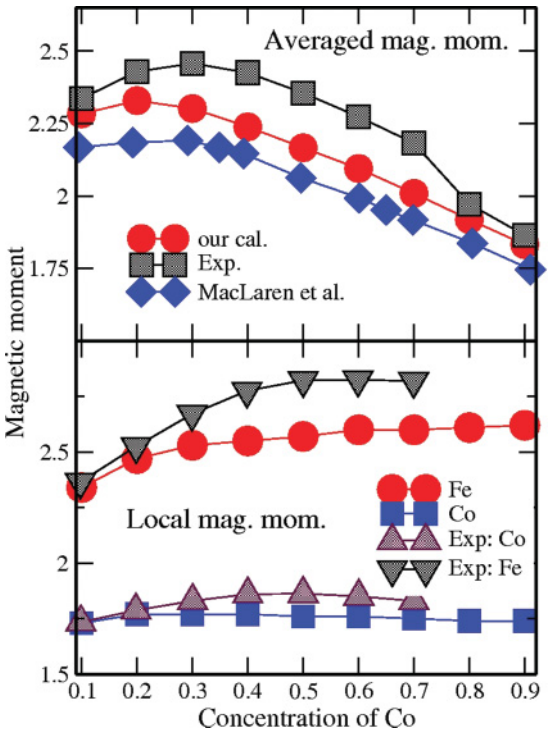

FIG. 3. (Color online) Magnetic moments of FeCo alloys. The experimental data have taken from Bardos (Ref. 46) and Collins and Forsythe (Ref. 45), and the theoretical data have been taken from MacLaren *et al.* (Ref. 43).

alloys exhibit the weakest environment effects compared to other Fe-based alloys. In addition, Co has small but significant orbital magnetism that makes the system more complicated.

According to the neutron-diffraction studies.[45] the complete occupation of the majority band of Fe by the addition of Co leads to a maximum mean magnetic moment 2.45 μ_B per atom at the composition $c_{\mathrm{Co}} = 0.3$. Figure 3 shows that our the KKR-CPA calculations reproduce well the experimental trend of magnetization with composition. One can notice quite a peculiar behavior of the local magnetic moments. The local moment on the Co atom remains nearly the same in the whole concentration range. At the same time, the local magnetic moment of Fe increases with increasing Co concentration from 2.2 μ_B in bcc Fe to the unusually large magnitude of about 2.62 μ_B at $c_{\mathrm{Co}} = 0.5$ and then remains almost constant. The addition of Co to Fe leads to a redistribution of the electrons such that the total system becomes a strong ferromagnet. The local moment of Fe is environment dependent. It increases with the number of Co nearest neighbors and takes its maximum value when all eight nearest-neighbor sites have been occupied by Co. This happens in the $B2$ structure.

B. Effective cluster interactions and ordering energies in the FM state

The effective cluster interactions in this work have been determined by the SGPM method. This method yields only a *chemical* contribution to the effective interactions, which determine the configurational energetics on a fixed ideal lattice. The contribution related to the possible local lattice relaxations should, however, be small in the Fe-Co alloys due to the small atomic-size mismatch of Fe and Co. We have also ignored contributions from lattice vibrations, which we expect to be insignificant in this system, at least relative to quite large chemical interactions.

The SGPM interactions are concentration and volume dependent. In Fig. 4, we show the EPI for three different alloy compositions: $Fe_{0.3}Co_{0.7}$, $Fe_{0.5}Co_{0.5}$, and $Fe_{0.7}Co_{0.3}$

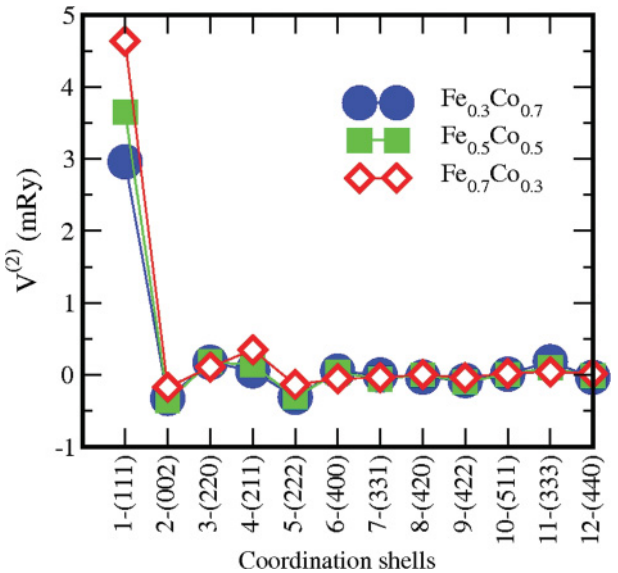

FIG. 4. (Color online) Composition variation of EPIs for the FM state Fe_xCo_{1-x} alloys.

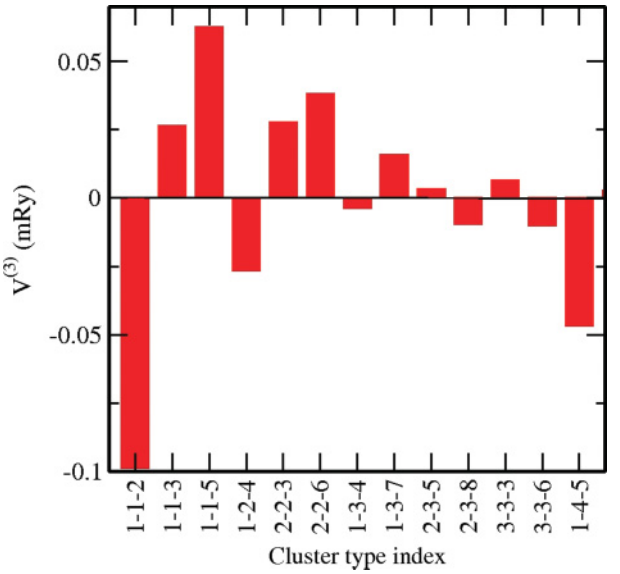

FIG. 5. (Color online) Three-site ECI for the $Fe_{0.5}Co_{0.5}$ alloy in the FM state.

in the FM state. As one can see, the strongest EPI is at the first coordination shell for all the alloy compositions. Other significant interactions are at the first five coordination shells and at the 11th coordination shell, which is in the closed-packed [111] direction. One can also notice that the nearest-neighbor EPI is changing almost by a factor of ∼1.68 in the concentration range of $0.3 < c_{\mathrm{Co}} < 0.7$, decreasing for Co-rich alloys. It is clear that such a dependence should affect the order-disorder transition temperature too.

We have also calculated the three- and four-site interactions. In Figs. 5 and 6 we show some of the strongest multisite interactions in the $Fe_{0.5}Co_{0.5}$ alloy in the ferromagnetic state.

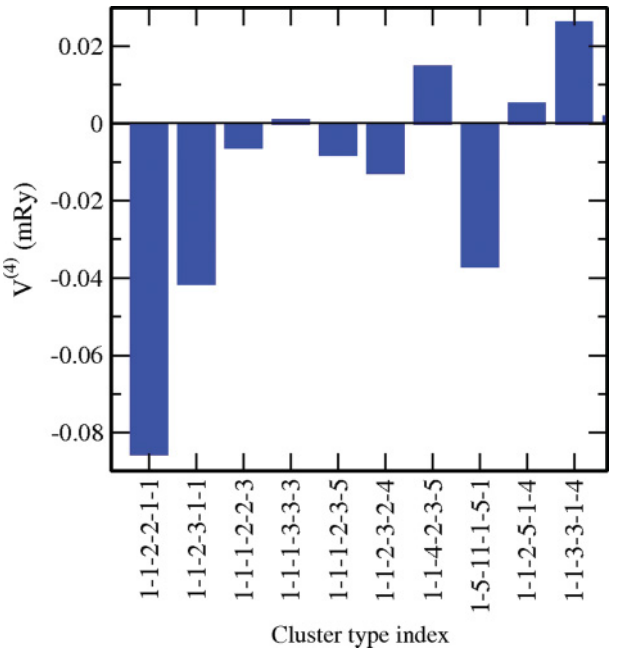

FIG. 6. (Color online) Four-site ECI for the $Fe_{0.5}Co_{0.5}$ alloy in the FM state.

TABLE I. The ordering energy calculated from the SGPM ECI and from the direct total energy calculations.

Structure	SGPM (mRy)	Total Energy (mRy)
$A11$	−0.231	−0.639
$B11$	0.200	0.649
$B2$	−5.051	−4.614
$B32$	0.634	0.509

The interaction index is given by the coordination shell numbers of the sides of the corresponding cluster. In the case of the four-site interactions, the order of indexes matters, so the choice is the following: the first four indexes are the coordination shells of the sides of a closed loop through all the four sites, and the last two are the coordination shells of remaining sides of the cluster. It is clear that many-body interactions do not vary systematically; however, in most cases, the strongest multisite interactions are along the line in the close-packed direction such as, for instance, $V^{(3)}_{1-1-5}$ in the case of three-site interactions and $V^{(4)}_{1-5-11-1-5-1}$ in the case of four-site interactions. The discussion of the trends for multisite ECI can be found in Ref. 48.

In order to check the validity of the SGPM effective cluster interactions, we have calculated the ordering energy of a set of ordered structures α, determined as the difference of the total energies of the ordered random alloys $\Delta E^{\alpha}_{\rm ord} = E^{\rm ord}_{\rm tot} - E^{\rm random}_{\rm tot}$ from both the direct total energy calculations using this formula as well as from the SGPM interactions. In Table I, we show the ordering energies of Fe-Co for four different ordered phases: $A11$, $B11$, $B2$, and $B32$. The agreement seems to be quite good, especially taking into consideration the fact that the SGPM interactions are obtained in the random state, where the magnetic state, including, for instance, the local magnetic moments of Fe and Co atoms, is different from those in the ordered structures.

C. Order-disorder phase transition in the reduced ferromagnetic state

Accurate phase equilibria calculations in magnetic systems become highly nontrivial at temperatures close to the point of a phase transition when magnetic and configurational interactions are of the same order, i.e., when magnetic and configurational degrees of freedom become strongly coupled and complexly interconnected. In Fe-Co alloys, the order-disorder phase transition is only 100 °C below the magnetic phase transition, which means that magnetic thermal excitations should affect the order-disorder phase transition.

Unfortunately, there is no simple and accurate first-principles-based approach to the description of the thermally excited ferromagnetic state of the itinerant magnets, such as Fe-Co alloys. Thus, the only way to proceed is to use a simplified model, hopefully not too simple, to describe the magnetic state. As has been mentioned above, we use the PDLM model for treating the alloy in the ferromagnetic state with a reduced magnetization. Since the magnetic excitations are much faster than atomic configuration, which is connected to the quite slow process of the atomic diffusion, we can separate out the magnetic degree of freedom. In the single-site mean-field consideration adopted in this work, the magnetic state is given by the reduced magnetization m.

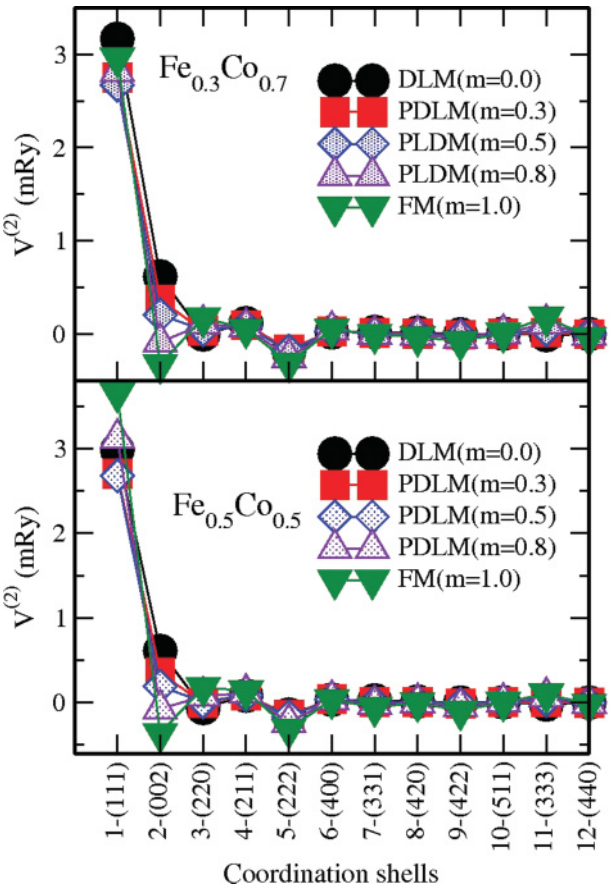

FIG. 7. (Color online) The magnetization-dependent EPIs of $Fe_{0.3}Co_{0.7}$ (upper panel) and $Fe_{0.5}Co_{0.5}$ (lower panel) alloys.

The variation of the EPI with magnetization from the DLM state ($m = 0$) to the FM state is shown in Fig. 7 for two different alloy compositions. It is clear that the mostly affected EPIs are for the first and second coordination shells. This is so because the connection between interactions in different magnetic states is roughly determined by the magnetic exchange interaction parameters, which have approximately the same hierarchy as the chemical interactions.[20] One can also see that the nearest-neighbor EPI changes nonmonotonically with magnetization. The most dramatic change with the magnetization is, however, for the next-nearest-neighbor EPI: it changes the sign from negative in the FM state to positive in the DLM state. In fact, this change in the EPI for the next nearest neighbor affects very strongly the order-disorder transition temperature.

The order-disorder transition temperatures in Fe-Co alloys in the concentration range of $0.3 < c_{\rm Co} < 0.7$ have been determined in the Monte Carlo simulations. The following ECI have been used in this case: The EPI at the first 30 coordination shells, 13 for three-site and 10 for four-site strongest ECI. In Fig. 8, we show the calculated order-disorder transition temperature of $Fe_{0.5}Co_{0.5}$ as a function of magnetization together with the EPI at the first five coordination shells. It is clear that transition temperature is very sensitive to the

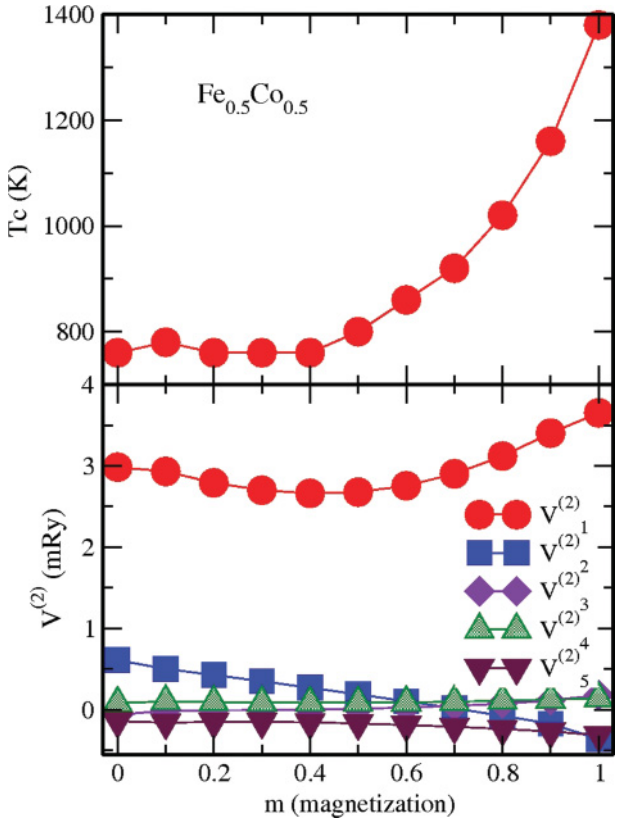

FIG. 8. (Color online) The order-disorder transition temperature (upper panel) and EPIs (lower panel) of the $Fe_{0.5}Co_{0.5}$ alloy as a function of magnetization.

magnetization. One can also see that the dependence of the transition temperature from the magnetic state is not entirely related to the magnetization dependence of the EPI at the first coordination shell. In fact, a very strong increase of the transition temperature close to the FM state is also related to the decrease of the EPI at the second coordination shell. This is so because the second coordination shell in the $B2$ structure consists of the atoms of the same type and, therefore, negative interaction at this coordination shell is stabilizing the $B2$ structure.

Finally, in Fig. 9, we show the calculated order-disorder transition temperature for several values of magnetization as function of alloy composition together with the experimental data.[3] The experimental transition temperature is close to the theoretical prediction for magnetization $m = 0.8$. There are very few experimental data for the magnetization close to the ordering transition. According an early experimental study by Clegg and Buckley,[49] and a Mössbauer study by Montano

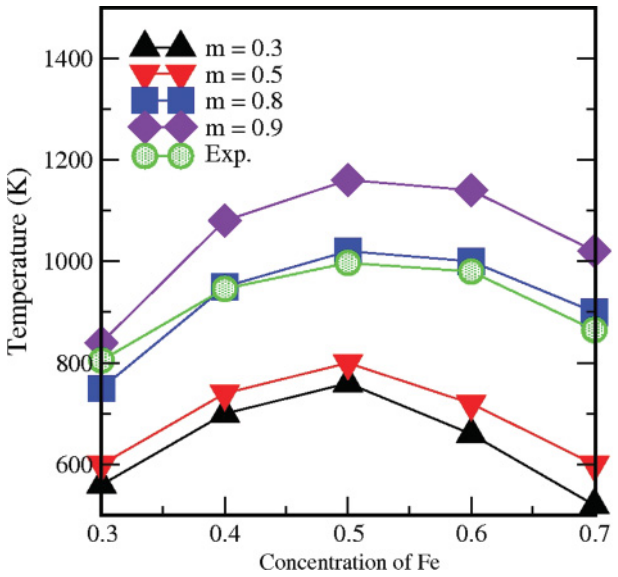

FIG. 9. (Color online) Concentration dependence of the transition temperature for different magnetizations.

and Seehra,[4] the magnetization at the temperature of the ordering transition is $m \simeq 0.83$ for the equiatomic alloy composition. Thus, one can conclude that our results are in very good agreement with experimental data.

Of course, such agreement can, to some degree, be fortuitous, and further investigations are apparently needed concerning the description of the magnetic state and probably some other contributions, which were neglected in this work. In particular, a drawback of our model is that it neglects longitudinal spin fluctuations expected to be important for Co-rich alloys. However, it is clear that our calculations confirm a quite strong dependence of the ordering effects on the degree of magnetization, similar to the cases of fcc Fe-Ni (Ref. 26) and bcc Fe-Cr alloys[25] considered lately.

ACKNOWLEDGMENTS

A.V.R. is grateful to the Swedish Research Council (VR) and the Swedish Foundation for Strategic Research (SSF) for financial support. M.R. would like to thank TWAS, Trieste, Italy, for partial financial assistance and I. A. Abrikosov, Department of Physics, Chemistry, and Biology (IFM), Linköping University, and Royal Institute of Technology, Stockholm, Sweden, for hospitality. Calculations have been done using UPPMAX (Uppsala), PDC (Stockholm), and NSC (Linköping) resources provided by the Swedish National Infrastructure for Computing (SNIC).

[1] T. Sourmail, Prog. Mater. Sci. **50**, 816 (2005).
[2] M. S. Seehra and P. Silinsky, Phys. Rev. B **13**, 5183 (1976).
[3] J. A. Oyedele and M. F. Collins, Phys. Rev. B **16**, 3208 (1977).
[4] P. A. Montano and M. S. Seehra, Phys. Rev. B **15**, 2437 (1977).
[5] D. Bonnenberg, K. A. Hempel, and H. P. J. Wijn, 1.2.1.1 Phase diagrams, Lattice parameters, edited by H. P. J. Wijn, Springer Materials–The Landolt-Bernstein Database.
[6] I. Ohnuma, H. Enoki, O. Ikeda, R. Kainuma, H. Ohtani, B. Sundman, and K. Ishida, Acta Mater. **50**, 379 (2002).

[7] V. Pierron-Bohnes, M. C. Cadeville, and F. Gautier, J. Phys. F: Met. Phys. **13**, 1889 (1983).
[8] V. Pierron-Bohnes, M. C. Cadeville, and F. Gautier, J. Phys. F: Met. Phys. **15**, 1441 (1985).
[9] V. Pierron-Bohnes, M. C. Cadeville, A. Bieber, and F. Gautier, J. Magn. Magn. Mater. **54**, 1027 (1986).
[10] A. Beinenstock and J. Lewis, Phys. Rev. **160**, 393 (1967).
[11] Z. Racz and M. F. Collins, Phys. Rev. B **21**, 229 (1980).
[12] R. A. Tahir-Kheli and T. Kawasaki, J. Phys. C **10**, 7207 (1977).
[13] L. Billard, P. Villemain, and A. Chamberod, J. Phys. C **11**, 2815 (1978).
[14] J. L. Morán-Lopez and L. M. Falicov, J. Phys. C **13**, 1715 (1980).
[15] F. Mejia-Lira, J. Urias, and J. L. Moŕan-Lopez, Phys. Rev. B **24**, 5270 (1981).
[16] J. Mizial, M. F. Collins, and M. Iwamatsu, J. Phys. F: Met. Phys. **12**, L115 (1982).
[17] J. M. Sanchez and C. H. Lin, Phys. Rev. B **30**, I448 (1984).
[18] F. J. Martinez-Herrera, F. Mejia-Lira, F. Aguilera-Granja, and J. L. Morán-Lopez, Phys. Rev. B **31**, 1686 (1985).
[19] F. Ducastelle and F. Gautier, J. Phys. F: Met. Phys. **6**, 2039 (1976).
[20] A. Bieber and F. Gautier, J. Magn. Magn. Mater. **99**, 293 (1991).
[21] M. Sluiter and Y. Kawazoe, Sci. Rep. Res. Inst., Tohoku Univ., Ser. A **40**, 301 (1995).
[22] J. Kudrnovský, I. Turek, A. Pasturel, R. Tetot, V. Drchal, and P. Weinberger, Phys. Rev. B **50**, 9603 (1994).
[23] A. Diaz-Ortiz, R. Drautzb, M. Fhnleb, and H. Doschb, J. Magn. Magn. Mater. **780**, 272 (2004).
[24] A. Diaz-Ortiz, R. Drautz, M. Fähnle, H. Dosch, and J. M. Sanchez, Phys. Rev. B **73**, 224208 (2006).
[25] A. V. Ruban, P. A. Korzhavyi, and B. Johansson, Phys. Rev. B **77**, 094436 (2008).
[26] M. Ekholm, H. Zapolsky, A. V. Ruban, I. Vernyhora, D. Ledue, and I. A. Abrikosov, Phys. Rev. Lett. **105**, 167208 (2010).
[27] M. Cyrot, Phys. Rev. Lett. **25**, 871 (1970).
[28] B. L. Gyorffy, A. J. Pindor. J. Staunton, G. M. Stocks, and H. Winter, J. Phys. F: Met. Phys. **15**, 1337 (1985).
[29] A. V. Ruban, S. Shallcross, S. I. Simak, and H. L. Skriver, Phys. Rev. B **70**, 125115 (2004).
[30] A. V. Ruban and H. L. Skriver, Phys. Rev. B **55**, 856 (1997).
[31] I. A. Abrikosov and H. L. Skriver, Phys. Rev. B **47**, 16532 (1993).
[32] A. V. Ruban and H. L. Skriver, Comput. Mater. Sci. **15**, 119 (1999).
[33] I. A. Abrikosov, A. M. N. Niklasson, S. I. Simak, B. Johansson, A. V. Ruban, and H. L. Skriver, Phys. Rev. Lett. **76**, 4203 (1996).
[34] I. A. Abrikosov, S. I. Simak, B. Johansson, A. V. Ruban, and H. L. Skriver, Phys. Rev. B **56**, 9319 (1997).
[35] L. Vitos, Phys. Rev. B **64**, 014107 (2001); L. Vitos, I. A. Abrikosov, and B. Johansson, Phys. Rev. Lett. **87**, 156401 (2001).
[36] P. Soven, Phys. Rev. **156**, 809 (1967).
[37] B. L. Gyorffy, Phys. Rev. B **5**, 2382 (1972).
[38] J. P. Perdew and Y. Wang, Phys. Rev. B **45**, 13244 (1992).
[39] A. V. Ruban and H. L. Skriver, Phys. Rev. B **66**, 024201 (2002).
[40] A. V. Ruban, S. Shallcross, S. I. Simak, and H. L. Skriver, Phys. Rev. B **70**, 125115 (2004).
[41] A. V. Ruban, S. I. Simak, P. A. Korzhavyi, and H. L. Skriver, Phys. Rev. B **66**, 024202 (2002).
[42] H. J. Monkhorst and J. D. Pack, Phys. Rev. B **13**, 5188 (1972).
[43] J. M. MacLaren, T. C. Schilthless, W. H. Butler, R. Sutton, and M. McHenry, J. Appl. Phys. **85**, 4833 (1999).
[44] A. V. Ruban, H. L. Skriver, and J. K. Norskov, Phys. Rev. Lett. **80**, 1240 (1998).
[45] M. F. Collins and J. B. Forsythe, Philos. Mag. **8**, 401 (1963).
[46] D. I. Bardos, J. Appl. Phys. **40**, 1371 (1969).
[47] M. C. Cadeville and J. L. Moran-Lopez, Phys. Rep. **153**, 331 (1987).
[48] A. Bieber and F. Gautier, J. Phys. Soc. Jpn. **53**, 2061 (1984).
[49] D. W. Clegg and R. A. Buckley, Met. Sci. **7**, 48 (1973).